A Three-stage Reliability Optimization Scheme For Hybrid AC/DC Distribution Systems

Runze Han, Tianyang Zhao
School of Electrical Engineering, Xi'an Jiaotong University, Xi'an, 710049, China
Hanrunze@stu.xjtu.edu.cn

***Abstract*—This paper proposes a three-stage reliability optimization scheme for hybrid AC/DC distribution networks to minimize load shedding during N-1 contingencies. The scheme leverages the operational flexibility of voltage source converters (VSCs) and inverter-based distributed generators (IBDGs) through fault isolation, microgrid reconfiguration, and recovery operations under utility coordination frameworks. A modified fictitious source bus concept ensures radial topology constraints during network partitioning. Case studies on a real 31-bus distribution network in southern China validate the proposed scheme, demonstrating 71.8% reduction in SAIFI and 49.5% reduction in SAIDI compared to traditional AC systems. Results validate the effectiveness of VSC-enhanced reliability optimization in hybrid networks.**

***Index Terms*—hybrid AC/DC, distribution networks, reliability, network reconfiguration**

I. INTRODUCTION

Reliability of distribution network is fundamental to ensuring continuous electricity supply to end users and represents a critical performance metric for modern power systems [1]. Increasing demands for uninterrupted power supply, driven by digitalization and electrification, have elevated reliability assessment to paramount importance in distribution network planning and operation [2]. Traditional reliability indices—System Average Interruption Frequency Index (SAIFI), System Average Interruption Duration Index (SAIDI), and Expected Energy Not Supplied (EENS)—have become industry standards for quantifying system performance and guiding investment decisions [3], [4].

Conventional reliability assessment methods for AC distribution networks include analytical and simulation-based approaches. Analytical methods, such as topology analysis and fault incidence matrix techniques, offer computational efficiency through closed-form expressions [5], [6]. However, these approaches are constrained to simple radial AC networks with limited operational flexibility. Simulation-based methods, particularly Monte Carlo techniques, provide enhanced modeling capabilities for capturing stochastic failures and dynamic variations [7]. Nevertheless, these approaches suffer from computational intensity and may converge to suboptimal solutions in large-scale or meshed networks [8].

The rapid integration of distributed energy resources, energy storage, and electric vehicles has led to the emergence of hybrid AC/DC distribution networks. These networks utilize voltage source converters (VSCs) as bidirectional interfaces, achieving superior energy conversion efficiency and flexible power flow control [9]. VSCs possess millisecond-level response characteristics that fundamentally differ from traditional protection devices, enabling rapid fault isolation and enhanced system observability [10], [11].

However, traditional methods lack analytical approaches specifically designed for hybrid AC/DC systems that can detail recovery processes and topology changes during faults. Moreover, multi-timescale characteristics require multi-stage analytical approaches rather than single-stage methods to accurately quantify recovery dynamics [12], [13].

The main contributions of this paper include:

- A novel three-stage reliability optimization scheme is proposed for hybrid AC/DC distribution networks, comprising fault isolation, microgrid reconfiguration, and system recovery. The framework fully utilizes the rapid control of VSCs and the flexibility of IBDGs, with each stage accurately modeled and interconnected by key time instants and constraints.
- A modified topology modeling method based on fictitious source buses and enhanced radial constraints is introduced, enabling reliable island identification and secure operation during microgrid reconfiguration, even under complex network partitioning.

This research focuses on technical feasibility analysis, assuming coordinated operation of IBDGs through utility coordination frameworks or grid code requirements, establishing the theoretical performance upper bound for hybrid AC/DC distribution networks.

II. THE FRAMEWORK OF THREE-STAGE SCHEME

This paper investigates reliability optimization scheme of hybrid AC/DC distribution networks with networked microgrids. The system consists of AC/DC distribution feeders interconnected by bidirectional VSCs that serve dual functions as subsystem interfaces and fault analysis information providers. Networked microgrids with IBDGs provide operational flexibility during normal and emergency conditions.

The proposed scheme employs a time-sequential three-stage analytical framework addressing the multi-timescale characteristics of hybrid systems. Critical time instants include: τ_{SW} (automated switching), τ_{TP} (tripping of the faulted line), and τ_{RP} (permanent repair), as illustrated in Fig. 1. Stage 1 (0 -

Supported by Smart Grid-National Science and Technology Major Project (2030) Pilot Project for Low-Carbon and High-Reliability Urban Distribution Power Systems (2024ZD0800700). Corresponding author: Tianyang Zhao.

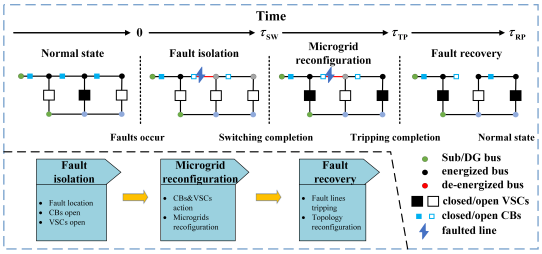

Fig. 1. Structure of the three-stage reliability enhancement scheme

τ_{SW}) implements minimum isolation boundary strategy where circuit breakers disconnect affected areas while VSCs are blocked to prevent damage, decomposing the network into isolated microgrids. Stage 2 (τ_{SW} - τ_{TP}) performs topology reconfiguration by activating backup connections and VSCs to supply outage areas through microgrids with IBDGs while maintaining radial constraints. Stage 3 (τ_{TP} - τ_{RP}) executes comprehensive topology optimization after manual fault removal to restore power to all recoverable loads. After the three stages, the faulted line is repaired and the distribution network will operate normally without load shedding.

III. Model Formulation

A. Objection Function

The objective of the three-stage model is to minimize load shedding under N-1 contingencies through topology reconfiguration. Therefore, the objective function consists of three components: load shedding penalties across all stages.

$$\min \quad \sum_{i\in \mathrm{V}} c_{\mathrm{LS}} \cdot \left(P^{\mathrm{FI}}_{\mathrm{LS},i} \cdot \tau_{\mathrm{SW}} + P^{\mathrm{MR}}_{\mathrm{LS},i} \cdot \tau_{\mathrm{TP}} + P^{\mathrm{TR}}_{\mathrm{LS},i} \cdot \tau_{\mathrm{RP}}\right) \quad (1)$$

where c_{LS} is the load shedding penalty coefficient.

B. First Stage: Fault Isolation

The fault isolation stage (0 - τ_{SW}) determines optimal switching actions to isolate faulted components. Decision variables are denoted with superscript FI.

1) Topological Constraints: In this stage, the model isolates faulted lines and affected buses while maintaining safe operation of the remaining system.

$$\begin{cases} f_{ij} \cdot \beta^{\mathrm{FI}}_{ij} \le z_i \\ f_{ij} \cdot \beta^{\mathrm{FI}}_{ij} \le z_j \end{cases}, \forall ij \in \mathrm{L} \cup \mathrm{L_{VSC}} \quad (2)$$

$$\begin{cases} z_i \le z_j + (1-\beta^{\mathrm{FI}}_{ij}) \\ z_i \ge z_j - (1-\beta^{\mathrm{FI}}_{ij}) \end{cases}, \forall ij \in \mathrm{L} \cup \mathrm{L_{VSC}} \quad (3)$$

$$\begin{cases} \beta^{\mathrm{FI}}_{ij} \le a_{ij} \\ \beta^{\mathrm{FI}}_{ij} \ge a_{ij} \cdot (1-r_{ij}) \end{cases}, \forall ij \in \mathrm{L} \cup \mathrm{L_{VSC}} \quad (4)$$

where $f_{ij} = 1$ indicates faulted line ij, and $r_{ij} = 1$ indicates line ij has CB or is VSC. Equation (2) ensures that both end buses of faulted lines without CB are placed in the fault zone. Equation (3) ensures that lines without CB/VSC remain closed, maintaining consistent fault status between connected buses. Equation (4) allows only CB-equipped lines and VSCs to open for fault isolation.

2) Operational Constraints: VSC power losses are modeled using rectifier power $P^{\mathrm{FI}}_{rec,i}$ (AC to DC) and inverter power $P^{\mathrm{FI}}_{inv,i}$ (DC to AC) with loss coefficient μ. Generation outputs are unified as $P^{\mathrm{FI}}_{\mathrm{G},i}$. For AC-side buses connected to VSCs, the power flowing from DC to AC side must account for VSC losses, with power balance constraints given by equation (5). For DC-side buses, the power balance constraints are expressed in equation (6).

$$\begin{cases} \sum\limits_{j:(i,j)\in \mathrm{L}} P^{\mathrm{FI}}_{ij} = P^{\mathrm{FI}}_{\mathrm{G},i} - P^{\mathrm{FI}}_{rec,i} + \mu \cdot P^{\mathrm{FI}}_{inv,i} \\ \qquad\qquad\qquad\qquad -(P_{d,i} - P^{\mathrm{FI}}_{\mathrm{LS},i}) \\ \sum\limits_{j:(i,j)\in \mathrm{L}} Q^{\mathrm{FI}}_{ij} = Q^{\mathrm{FI}}_{\mathrm{G},i} - Q^{\mathrm{FI}}_{rec,i} + \mu \cdot Q^{\mathrm{FI}}_{inv,i} \\ \qquad\qquad\qquad\qquad -(Q_{d,i} - Q^{\mathrm{FI}}_{\mathrm{LS},i}) \end{cases}, \quad \forall i \in \mathrm{V} \quad (5)$$

$$\begin{cases} \sum\limits_{j:(i,j)\in \mathrm{L}} P^{\mathrm{FI}}_{ij} = P^{\mathrm{FI}}_{\mathrm{G},i} - \mu \cdot P^{\mathrm{FI}}_{rec,i} + P^{\mathrm{FI}}_{inv,i} \\ \qquad\qquad\qquad\qquad -(P_{d,i} - P^{\mathrm{FI}}_{\mathrm{LS},i}) \\ \sum\limits_{j:(i,j)\in \mathrm{L}} Q^{\mathrm{FI}}_{ij} = Q^{\mathrm{FI}}_{\mathrm{G},i} - \mu \cdot Q^{\mathrm{FI}}_{rec,i} + Q^{\mathrm{FI}}_{inv,i} \\ \qquad\qquad\qquad\qquad -(Q_{d,i} - Q^{\mathrm{FI}}_{\mathrm{LS},i}) \end{cases}, \quad \forall i \in \mathrm{V} \quad (6)$$

For buses within the fault zone, all loads must be shed.

$$\begin{cases} P^{\mathrm{FI}}_{\mathrm{LS},i} - P_{\mathrm{L},i} \le M \cdot (1 - z^{\mathrm{FI}}_i) \\ P^{\mathrm{FI}}_{\mathrm{LS},i} - P_{\mathrm{L},i} \ge -M \cdot (1 - z^{\mathrm{FI}}_i) \\ Q^{\mathrm{FI}}_{\mathrm{LS},i} - Q_{\mathrm{L},i} \le M \cdot (1 - z^{\mathrm{FI}}_i) \\ Q^{\mathrm{FI}}_{\mathrm{LS},i} - Q_{\mathrm{L},i} \ge -M \cdot (1 - z^{\mathrm{FI}}_i), \end{cases} \quad \forall i \in \mathrm{V} \quad (7)$$

Additional operational constraints follow standard formulations in [14], with DC line voltage constraints considering resistance only.

C. Second Stage: Microgrid Reconfiguration

The microgrid reconfiguration stage (τ_{SW} - τ_{TP}) performs emergency reconfiguration after fault isolation. CBs decompose the network into microgrids, which are reconfigured via backup lines and VSCs to restore loads using available IBDGs. Decision variables use superscript MR.

1) Topological Constraints: The reconfiguration determines optimal switching to form autonomous microgrids.

$$1 - \beta^{\mathrm{MR}}_{ij} \ge \alpha_{ij} - \beta^{\mathrm{MR}}_{ij}, \forall ij \in \mathrm{L} \cup \mathrm{L_{VSC}} \quad (8)$$

$$z^{\mathrm{FI}}_i(1-z^{\mathrm{FI}}_j) + z^{\mathrm{FI}}_j(1-z^{\mathrm{FI}}_i) \le 1 - \beta^{\mathrm{MR}}_{ij}, \quad \forall ij \in \mathrm{L} \cup \mathrm{L_{VSC}} \quad (9)$$

$$\beta^{\mathrm{FI}}_{ij} - r_{ij} \le \beta^{\mathrm{MR}}_{ij} \le \beta^{\mathrm{FI}}_{ij} + r_{ij}, \quad \forall ij \in \mathrm{L} \cup \mathrm{L_{VSC}} \quad (10)$$

where equation (8) keeps switches opened in stage 1 remain open. Equation (9) prevents unsafe connections between

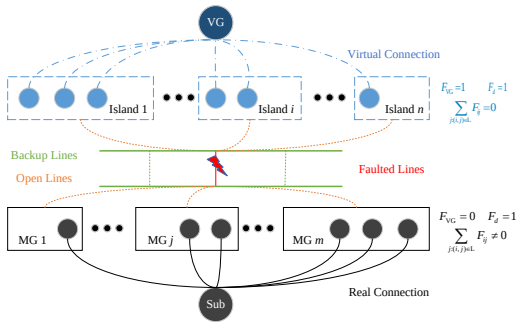

Fig. 2. Fictitious source bus and microgrid area

faulted and healthy zones. Equation (10) allows only CB-equipped lines and VSCs to change status.

When backup lines are closed for microgrid reconfiguration, the distribution network must be radial. Traditional radial topology constraints [15] assume each non-substation buses has a fictitious load $F_d = 1$, enforcing radial topology through fictitious power flow constraints that establish the relationship between topology and bus/line states. However, when terminal lines are disconnected, terminal buses lose all power supply paths and cannot be supplied with fictitious power, rendering traditional fictitious power flow constraints inapplicable.

To address this challenge, we introduce a fictitious source bus VG with fictitious power output $F_{\text{VG}} = 1$, to which all islanded buses that lose connection with substation buses are connected. The modified fictitious power flow constraint becomes:

$$\sum_{j:(i,j)\in \text{L}} F_{ij}^{\text{MR}} = F_{\text{G},i}^{\text{MR}} + F_{\text{VG},i}^{\text{MR}} - F_{d,i}, \quad \forall i \in \text{V} \tag{11}$$

$$-S_{\max}\beta_{ij}^{\text{MR}} \le F_{ij}^{\text{MR}}, F_{\text{VSC},ij}^{\text{MR}} \le S_{\max}\beta_{ij}^{\text{MR}}, \forall ij \in \text{L} \cup \text{L}_{\text{VSC}} \tag{12}$$

However, even with identified islanded buses disconnected from substations, determining the number of islands they form remains challenging, making it impossible to construct proper bus-line radial constraints. Therefore, we introduce binary variable $I_{s,ij}^{\text{MR}}$. When line ij is closed and both $F_{\text{VG},i} = F_{\text{VG},j} = 1$, it indicates that buses i and j belong to the same island. The enhanced radial topology constraint becomes:

$$\sum_{ij\in \text{L}} \beta_{ij}^{\text{MR}} = N_d - N_g - \sum_{i\in \text{V}} F_{\text{VG},i}^{\text{MR}} + \sum_{ij\in \text{L}} I_{s,ij}^{\text{MR}} \tag{13}$$

$$\begin{cases} I_{s,ij}^{\text{MR}} & \le F_{\text{VG},i}^{\text{MR}} \\ I_{s,ij}^{\text{MR}} & \le F_{\text{VG},i}^{\text{MR}} \\ I_{s,ij}^{\text{MR}} & \le \beta_{ij}^{\text{MR}} \\ I_{s,ij}^{\text{MR}} & \ge F_{\text{VG},i}^{\text{MR}} + F_{\text{VG},i}^{\text{MR}} + \beta_{ij}^{\text{MR}} - 2 \end{cases} \quad \forall i,j \in \text{V} \tag{14}$$

where N_d is the total number of buses, n_g is the number of substation buses, and $I_{s,ij}^{\text{MR}}$ is the binary variable identifying island lines. Equations (13)-(14) ensure the correct logical relationship for $I_{s,ij}^{\text{MR}}$: it equals 1 only when the line is closed and both end buses are connected to the fictitious source, effectively capturing the island structure for radial topology enforcement.

2) Operational Constraints: Operational constraints are similar to equations (5)-(12) and are omitted for brevity.

D. Third Stage: Fault Repair

The fault repair stage (τ_{TP} - τ_{RP}) represents the recovery period where faulted components are permanently removed and the network is reconfigured to restore power supply. Since faulted lines are eliminated, no fault zones exist in the system. Decision variables use superscript FR.

The reconfiguration optimizes switching actions to achieve the best network topology without faulted components. The key constraint is:

$$\beta_{\text{fault}}^{\text{FR}} = 0 \tag{15}$$

which ensures permanent removal of the faulted line.

The remaining constraints are similar to equations (5)-(12) and (11)-(14) as the first and second stage, and are omitted here for brevity.

E. Reliability Index Calculation

Based on the three-stage reliability optimization results, we can evaluates hybrid AC/DC distribution network reliability using traditional indices: System Average Interruption Frequency Index (SAIFI), System Average Interruption Duration Index (SAIDI), and Expected Energy Not Served (EENS).

1) bus-Level Reliability Indices: For each load bus i experiencing line k fault, the reliability indices are:

Customer Interruption Frequency (CIF):

$$CIF_{i,k} = \lambda_k \cdot I_{i,k}^{\text{FI}} \tag{16}$$

Customer Interruption Duration (CID):

$$CID_{i,k} = \lambda_k \cdot \left(I_{i,k}^{\text{FI}} \cdot \tau_{\text{SW}} + I_{i,k}^{\text{MR}} \cdot (\tau_{\text{TP}} - \tau_{\text{SW}})\right) \tag{17}$$

Expected Energy Not Served (EENS):

$$EENS_{i,k} = \lambda_k \cdot \left(P_{\text{LS},i,k}^{\text{FI}} \cdot \tau_{\text{SW}} + P_{\text{LS},i,k}^{\text{MR}} \cdot (\tau_{\text{TP}} - \tau_{\text{SW}})\right) \tag{18}$$

where λ_k is the failure rate of line k (failures/year). $P_{\text{LS},i,k}$ is the load shedding amount at bus i during each stage when line k fails. $I_{i,k}$ is the outage indicator variable, equal to 1 when $P_{\text{LS},i,k} > 0$, otherwise 0.

2) System-Level Reliability Indices: Aggregating all $N-1$ line fault scenarios:

System Average Interruption Frequency Index (SAIFI):

$$SAIFI = \frac{\sum_{i=1}^{N_d} CIF_i \cdot NC_i}{\sum_{i=1}^{N_d} NC_i} \tag{19}$$

System Average Interruption Duration Index (SAIDI):

$$SAIDI = \frac{\sum_{i=1}^{N_d} CID_i \cdot NC_i}{\sum_{i=1}^{N_d} NC_i} \tag{20}$$

System Expected Energy Not Served (EENS):

$$EENS_{sys} = \sum_{i=1}^{N_d} \sum_{k=1}^{N_l} EENS_{i,k} \tag{21}$$

where

$$CIF_i = \sum_{k=1}^{N_l} CIF_{i,k} \tag{22}$$

$$CID_i = \sum_{k=1}^{N_l} CID_{i,k} \tag{23}$$

NC_i is the number of customers at bus i, N_d is the total number of load buses, and N_l is the total number of lines (including AC lines, DC lines, and VSCs).

F. Computational Complexity Analysis

The proposed three-stage reliability optimization scheme involves solving sequential mixed-integer linear programming (MILP) problems with manageable computational complexity.

Problem Scale: For a hybrid AC/DC distribution network with n_b buses, n_l AC lines, n_{vsc} VSC connections, n_g generators, and n_{dg} IBDGs:

- **Stage 1:** $(n_b + n_l + n_{vsc})$ binary + $(3n_b + 2n_l + 2n_g + 2n_{dg} + 2n_{vsc})$ continuous variables, $2n_b$ equality constraints + $(2n_b + 14n_l + 2n_g + 2n_{dg} + 14n_{vsc})$ inequality constraints
- **Stage 2:** $(n_b + 2n_l + 2n_{vsc} - n_g)$ binary + $(3n_b + 3n_l + 3n_g + 2n_{dg} + 3n_{vsc})$ continuous variables, $(3n_b + 1$ equality constraints + $(2n_b + 8n_l + 2n_g + 2n_{dg} + 8n_{vsc})$ inequality constraints
- **Stage 3:** Same number of variables as Stage 2, $(3n_b + 2)$ equality constraints + $(2n_b + 10n_l + 2n_g + 2n_{dg} + 10n_{vsc})$ inequality constraints

The total number of variables and constraints across all stages is $\mathcal{O}(n_b + n_l + n_g + n_{mg} + n_{vsc})$, which scales linearly with the network size.

IV. Case Study

A. Description

The proposed three-stage reliability assessment framework is validated using a real hybrid AC/DC distribution network from a southern Chinese city. This system represents a typical modern urban distribution network integrating renewable energy sources and DC microgrids, as illustrated in Fig. 3. The system features DC buses at 11-13, 16, and 31, which connect to the AC network through VSCs. To maintain the required radial topology for normal distribution operation, only VSCs on lines 8-11, 14-16, and 25-31 remain closed under normal conditions, while other VSCs serve as backup connections. The network includes both grid-forming and grid-following IBDGs strategically positioned to enhance operational flexibility during normal and emergency conditions. Reliability parameters are set based on actual utility operational data: $\tau_{\text{SW}} = 60s$ (automated switching), $\tau_{\text{TP}} = 100s$ (tripping of the faulted line), $\tau_{\text{RP}} = 1h$ (permanent repair), representing typical response times in this urban distribution environment.

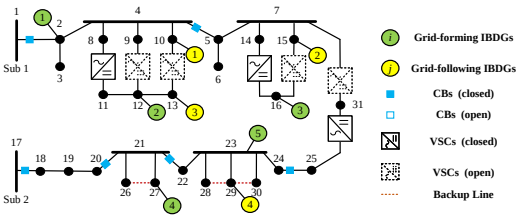

Fig. 3. A real hybrid AC/DC distribution network in a southern Chinese city

B. Fault Scenarios and Three-Stage Analysis

To demonstrate the proposed three-stage scheme, a critical fault scenario is analyzed involving permanent line failure and subsequent recovery processes.

As illustrated in Fig. 4(a), a permanent fault occurs on line 2-4. Following equations (2)-(4), CBs on lines 1-2 and 4-5 open immediately to prevent fault propagation. Simultaneously, the VSC on line 8-11 detects excessive short-circuit currents and enters blocking mode to prevent equipment damage. With CBs and VSCs disconnected, the distribution network decomposes into multiple zones: the red zone represents the fault area where all loads are shed. The blue zones are islanded microgrids that lose connection to the substation. Microgrids with IBDGs can supply internal loads, while the others lose all their loads. The green zone contains the substation and has no load interruption.

After the switching time delay τ_{SW}, topology reconfiguration begins as shown in Fig. 4(b). The VSC (or backup lines) between buses 7-31 closes to reconnect the islanded blue microgrids to the main grid. This reconfiguration enables recovery of loads at buses 5-7 and 14-16, which might be de-energized previously. The VSC between buses 8-11 remains blocked to maintain system stability, while the fault area continues isolation pending tripping the faulted line.

The final stage, depicted in Fig. 4(c), involves manual disconnection of the faulted line 2-4 and establishment of alternative connection paths. Network reconfigure to create a new radial topology that restores power supply to all previously affected areas while maintaining fault isolation. This demonstrates the framework's capability to minimize outage duration throughout the recovery process.

C. Comparative Analysis

To validate the effectiveness of the proposed three-stage reliability enhancement framework, three comparative cases are established for comprehensive analysis. Table I presents the reliability performance comparison across different network configurations:

Case 1: Traditional AC distribution network using single-stage restoration methods without VSC capabilities.

Case 2: Hybrid AC/DC distribution network implementing the three-stage scheme with limited VSC deployment.

Case 3: Hybrid AC/DC distribution network implementing the three-stage scheme with full VSC integration.

The conventional AC distribution network exhibits the poorest reliability performance across all metrics (Case 1). When

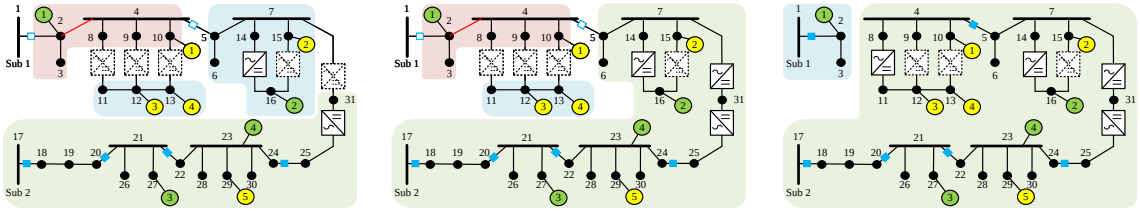

a) Fault isolation in the first stage b) Microgrid reconfiguration in the second stage c) Fault restoration in the third stage

Fig. 4. The three-stage recovery process under the fault scenario

TABLE I
RELIABILITY PERFORMANCE COMPARISON

Reliability Index	AC	AC/DC & limited VSCs	AC/DC
SAIFI (failures/year)	1.1059	0.4647	0.3118
SAIDI (minutes/year)	1.2353	0.7765	0.6235
EENS (kWh/year)	34.9587	17.6667	14.167

line 2-4 fault, over-current protection trips CB 1-2, causing all downstream buses (2-16) to lose power. After fault location is completed, switch 4-5 receives the opening command but requires switching time τ_{SW} to actually open. Only after line 4-5 opens can buses 5-7 and 14-16 be outside the fault zone and restored, while buses 2-4 remain isolated. This extended outage area and duration results in the highest metrics.

Case 2 represents a compromise design with limited VSC backup (only VSC 8-11 configured), yielding intermediate reliability performance. The critical vulnerability lies in the failure risk of the only VSC. When VSC 8-11 fails, the DC microgrid becomes completely isolated, causing extended outages lasting the entire VSC repair duration (τ_{RP}). This concentrated dependency creates higher vulnerability compared to distributed VSC backup.

Hybrid AC/DC network implementing the three-stage scheme with comprehensive VSC backup (Case 3) demonstrates superior reliability performance, achieving 71.8% reduction in SAIFI, 49.5% reduction in SAIDI and 59.5% reduction in EENS. This improvement stems from VSCs' ability to detect fault currents and enter blocking mode within milliseconds, eliminating extended fault location procedures. Additionally, DC microgrids can maintain autonomous operation through local IBDGs during fault isolation to reduce load curtailment.

V. CONCLUSION

This paper presents a three-stage reliability optimization scheme for hybrid AC/DC distribution networks to enhance system reliability. The proposed scheme leverages VSCs' rapid response capabilities and microgrid reconfiguration to minimize load shedding during N-1 contingencies.

Comparative reliability analysis demonstrates significant performance improvements over traditional AC distribution systems. The comprehensive backup configuration of VSC achieves a reduction of 71. 8% in SAIFI, a reduction of 49. 5% in SAIDI and a reduction of 59. 5% in EENS. These improvements stem from VSCs' millisecond-level fault isolation, elimination of extended fault location procedures, and enhanced DC microgrid autonomy during disturbances.

REFERENCES

[1] Q. Xu, T. Zhao, Y. Xu, Z. Xu, P. Wang and F. Blaabjerg, "A Distributed and Robust Energy Management System for Networked Hybrid AC/DC Microgrids," in IEEE Transactions on Smart Grid, vol. 11, no. 4, pp. 3496-3508, July 2020.

[2] C. Chen, J. Wang, F. Qiu and D. Zhao, "Resilient Distribution System by Microgrids Formation After Natural Disasters," in IEEE Transactions on Smart Grid, vol. 7, no. 2, pp. 958-966, March 2016.

[3] A. Arefi, G. Ledwich, G. Nourbakhsh and B. Behi, "A Fast Adequacy Analysis for Radial Distribution Networks Considering Reconfiguration and DGs," in IEEE Transactions on Smart Grid, vol. 11, no. 5, pp. 3896-3909, Sept. 2020.

[4] "IEEE Guide for Electric Power Distribution Reliability Indices," in IEEE Std 1366-2022 (Revision of IEEE Std 1366-2012) , vol., no., pp.1-44, 22 Nov. 2022.

[5] J. Zhang, B. Wang, H. Ma, Y. He, Y. Wang, and Z. Xue, "Reliability Evaluation of Cabled Active Distribution Network Considering Multiple Devices—A Generalized MILP Model," Processes, vol. 11, no. 12, pp. 3404, Dec. 2023.

[6] F. Luo, N. Ge and J. Xu, "Analytical Calculation Method for Power Supply Reliability of Distribution Systems With Multiple Tie Lines," in IEEE Transactions on Reliability.

[7] M. Omri, M. Jooshaki, A. Abbaspour and M. Fotuhi-Firuzabad, "Modeling Microgrids for Analytical Distribution System Reliability Evaluation," in IEEE Transactions on Power Systems, vol. 39, no. 5, pp. 6319-6331, Sept. 2024.

[8] M. M. Breve, B. Bohnet, and G. Michalke, "Flow-network-based method for the reliability analysis of decentralized power system topologies with a sequential Monte-Carlo simulation," IEEE Trans. Power Syst., vol. 38, no. 6, pp. 5234-5247, 2023.

[9] M. Shahbazi, "An Efficient Universal AC/DC Branch Model for Optimal Power Flow Studies in Hybrid AC/DC Systems," IEEE Trans. Power Syst., 2024.

[10] J. Zhang, Y. Ji, J. Zhou, Y. Jia, and G. Shi, "Cooperative AC/DC Voltage Margin Control for Mitigating Voltage Violation of Rural Distribution Networks with Interconnected DC Link," IEEE Trans. Power Syst., vol. 40, no. 2, pp. 1234-1245, 2025.

[11] W. Lambrichts and M. Paolone, "General and Unified Model of the Power Flow Problem in Multiterminal AC/DC Networks," IEEE Trans. Power Syst., 2024.

[12] Chen, Youhong. Stability Assessment of Power Systems with Multiple Voltage Source Converters: Bifurcation-Theory-Based Methods. Springer Nature, 2024.

[13] B. Chen, Y. Zhang, H. Liang, "Multi-Level Network Topology and Time Series Multi-Scenario Optimization Planning Method for Hybrid AC/DC Distribution Systems in Data Centers," Electronics, vol. 14, no. 2, p. 264, 2025.

[14] Z. Wang, T. Ding, X. Zhang, C. Mu, P. Du and F. Li, "Multi-Period Resilient Model for VSC-Based AC-DC HDS Considering Public-Safety Power Shutoff to Mitigate Wildfires," in CSEE Journal of Power and Energy Systems, vol. 10, no. 2, pp. 821-833, March 2024.

[15] Y. Bian, Z. Bie and G. Li, "Proactive repair crew deployment to improve transmission system resilience against hurricanes," in IET Generation, Transmission & Distribution 15(5): 870-882, Dec. 2020.